INVESTIGATING THE USE OF CHITOSAN AS A COUPLING AGENT TO IMPROVE THE INTERFACIAL PROPERTIES OF PHOSPHATE GLASS FIBRE/POLYCAPROLACTONE COMPOSITES

Chao Tan[1], Ifty Ahmed[2], Andrew J. Parsons[2], Chenkai Zhu[1], Junxiao Zhang[1], Chris D. Rudd[1, 2] and Xiaoling Liu[1]*

[1] The University of Nottingham Ningbo China, Ningbo, 315100, China
[2] The University of Nottingham, Nottingham, NG7 2RD, U.K.
* Corresponding author at Science and Engineering Building, the University of Nottingham Ningbo China, Ningbo, 315100, China. Tel: +86 (0)574 8818 0000 (Ext 8057), Email: Xiaoling.Liu@nottingham.edu.cn

Keywords: Coupling agents, Chitosan, Phosphate glass fibres, Polycaprolactone composites, Interfacial properties

ABSTRACT

Chitosan (CS) was investigated to improve the interfacial properties of the phosphate glass fibre/polycaprolactone (PGF/PCL) composites. Dilute acetic acid was used as the solvent for CS and its influence on mechanical properties of the fibres was analysed via single fibre tensile testing. The interfacial shear stress (IFSS) was analysed using a fragmentation test and the interaction between the sizing agent and the glass surface was analysed by XPS. TGA and SEM were also used to indicate the sizing performance. A dip-coating process in the CS-acetic acid solution was observed to increase the IFSS by 56% with insignificant ($p > 0.05$) fibre strength loss compared to the pure PGF control. The enhancement of IFSS after sizing was suggested to be attributed to the interaction between the protonated amine groups of the CS and the phosphate structure of the PGF. Then the sized fibres were rinsed in the acetic acid solution (2% v/v) to remove the extra agent on the fibre surface and the IFSS consequently increased by 78% of the control, but with a significant ($p < 0.001$) strength loss of 20%. This increase in IFSS was suggested to be due to the improvement of the interphase and load transmission between the matrix and fibres.

1 INTRODUCTION

Phosphate glass fibre (PGF) stands out as a reinforcing fibre due to its ability to dissolve completely in aqueous media, with tailorable durability via the addition of metal oxides [1-4], with sufficient mechanical strength for bone repair [5] and good body tolerance [6-8]. Much work so far has focused on PGF/polymer composites as a substitute of conventional metal alloy-based bone fracture fixation devices [5, 9, 10]. However, the application of these composites, such as PGF/PCL [2, 11], is limited by a rapid loss of strength after exposure to an aqueous physiological environment, which is suggested to be due to degradation of the fibre/matrix interface [12, 13]. Coupling agents have been studied to enhance the hydrolytic stability of this interface [14, 15].

Chitosan (CS) is the second most abundant of the natural polysaccharides next to cellulose and it has generated enormous interest due to its biodegradability and biocompatibility [16, 17]. Moreover, the reactive functional groups (hydroxyls, acetamides and amines [18-20]) make CS outstanding in the bio-composite field, such as blending [21, 22], organic coupling agents [23, 24], nanocomposites [25] and reinforced collagen structures [18, 26]. However, to the author's best knowledge, no study has been published on CS as a coupling agent to improve the interface of PGF/PCL composites. Not only the investigation of CS/PCL blends [27, 28], but also the production of CS/phosphate glass composites [26, 29] give evidence that CS has a good interaction with PCL and PGF and has the potential to be a successful coupling agent in PGF/PCL composites.

It was expected that CS would interact with PGF via hydrogen, P-O-C and/or N-P bonding. Acetic acid would be used as the solvent of CS [30], which might impact the mechanical properties of PGF. However, this impact could be controlled via sizing time and concentration. Additionally, the acid might roughen the PGF surface and physically enhance the interface of the composites. This study investigated the feasibility of CS as a coupling agent to enhance the interfacial properties of PGF/PCL composites, as well as the influence of immersion in the acetic acid solution. Mechanical properties of the sized and unsized fibres were measured. The interfacial shear stress (IFSS) was analysed using a single fibre fragmentation test. TGA was performed to quantify the amount of sizing agents present on the fibres and XPS analysis was conducted to investigate the interaction between CS and PGF. Morphologic examination was also performed via SEM to observe the sizing performance.

2 MATERIALS AND METHODS

2.1 Phosphate glass and fibre production

Phosphate-based glass ($45P_2O_5$-$5B_2O_3$-$5Na_2O$-24CaO-10MgO-$11Fe_2O_3$ in mol%) was prepared and its composition was confirmed by inductively coupled plasma mass spectrometry (ICP-MS, Thermo Scientific iCAP Qc, UK) [4]. Continuous fibres of ~25 μm diameter were produced via a melt-draw spinning process using a dedicated in-house facility [31].

2.2 Sizing application

The sizing solution was was prepared by dissolving 0.3g CS powder (low Mw, DD > 80%, Sigma-Aldrich, USA) into 100 mL 2% v/v acetic acid solution and stirring at room temperature using a magnetic stirrer (IKA, Germany) with a PTFE rotor until a transparent viscous solution was obtained. About 0.2 g PGFs of 100 mm long were then dip-coated in the solution as detailed in Table 1.

Table 1: Details of sizing application processes. The unsized PGF was prepared as a control. The sample codes were also used for the corresponding single fibre composites (SFCs).

Sample codes		PGF	PGF/CS-3R	PGF/CS-3
Acetic acid solution (2% v/v)	[mL]	-	100	100
CS (low Mw, DD > 80%)	[g]	-	0.3	0.3
Stirring	[hour]	-	2	2
PGF dip-coating (pH 2.99, 24.0℃)	[min]	-	30	30
PGF/CS dried at RT	[hour]	-	2	2
PGF/CS rinsed by acetic acid solution (2% v/v)	[min]	-	30	-
PGF/CS dried at 50 °C	[hour]	24	24	24

2.3 Single fibre tensile test (SFTT)

The tensile properties of the fibres were obtained using a LEX 820 tensile tester (Diastron, UK), in accordance with ISO 11566 [31]. 30 samples were prepared at a gauge length of 25 mm for each treatment type. The crosshead speed of the machine was 0.017 mm s^{-1} and the load cell capacity was 1 N. PGFs are essentially brittle and Weibull distribution is an accepted statistical tool used to characterise the failure mode of brittle fibres [12]. In this study, Weibull parameters were obtained from the tensile strength data calculated using Minitab 17.

2.4 Single fibre fragmentation test (SFFT)

SFC specimens were produced by placing an axially aligned single fibre between two rectangular pieces of PCL film of 75 × 25 × 0.2 mm^3 and hot pressing at 120 °C under 14 bar for 10 min. The

resulting specimens were cooled to room temperature and finally cut into dog-bone shapes. These were axially loaded in a MTS E45 tensile testing machine (USA) with a load cell of 1 kN and a crosshead speed of 1 mm min^{-1} until obtained an axial extension of 25%. After having conducted the fragmentation, the specimens were placed under an optical microscope (NE 930, Nexcope, China) and the number of fibre fragments present in the 25mm gauge length were counted for the calculation of IFSS.

The IFSS values were calculated using the Kelly-Tyson equation [12]:

$$\tau = \frac{\sigma_f \cdot d}{2 \cdot l_c} \tag{1}$$

where τ is the IFSS, d is the fibre diameter, σ_f is the single fibre tensile strength at the critical fragment length l_c.

$$\sigma_f = \sigma_0 \cdot \left(\frac{l_c}{l_0}\right)^{-1/m} \tag{2}$$

$$l_c = \frac{4}{3} \cdot l_f \tag{3}$$

$$l_f = \frac{l_0}{N} \tag{4}$$

where σ_0 and m are the Weibull scale and shape parameter respectively, for the fibre strength at gauge length l_0, l_f is the average fragment length and N is the number of fibre fragments obtained from optical microscopy [12].

2.5 Scanning electron microscopy (SEM)

Chopped fibres were fixed on the sample stage with conductive adhesive tape and then coated with gold using a Leica EM SCD 500 high vacuum sputter coater (Germany). The stage with sample was placed into a Zeiss Sigma/VP SEM (Germany).

2.6 Thermogravimetry (TG)

TG analysis was performed to quantify the amount of sizing agents present on the fibre surfaces. The analyses were conducted from room temperature to 1000 °C for CS powders and to 500 °C for sized and unsized fibres, using an SDT Q600 thermogravimetric analyser from TA instruments (USA) with a heating rate of 20 °C min^{-1} in flowing nitrogen gas of 50 mL min^{-1}.

2.7 X-ray photoelectron spectroscopy (XPS)

X-ray photoelectron spectroscopy (XPS) analysis investigated the effectiveness of sizing agent application to the fibre surfaces. A Kratos Axis Ultra with a monochromated Al ka X-ray source (1486.6 eV) was operated at 8 mA emission current and 12 kV anode potential. For the XPS measurement, a small batch of fibres was mounted on a hollow steel bar using a conductive adhesive tape at two ends, while CS powders were adhered by the conductive tape on the steel bar. Drift of the electron binding energy of the peaks due to a surface charging effect was calibrated by utilising the C_{1s} peak of the contamination (284.8 eV).

2.8 Statistical analysis

Statistical analysis was performed using the IBM SPSS (version 22). A Student's unpaired t-test was used to analyse the significance of difference between different samples, assuming equal variance and determining two-tailed *p* values.

3 RESULTS

3.1 Mechanical properties of fibres

A significant tensile strength loss of 20.2% ($p < 0.001$) was found for the PGF/CS-3R fibres compared to the control (PGF), while an insignificant decrease ($p > 0.05$) of 7.5% was obtained from the control to the PGF/CS-3 fibres (see Figure 1). Table 2 represents the Weibull distribution of tensile strength. It was noted that the trend of normalising strength was consistent with that of mean tensile strength.

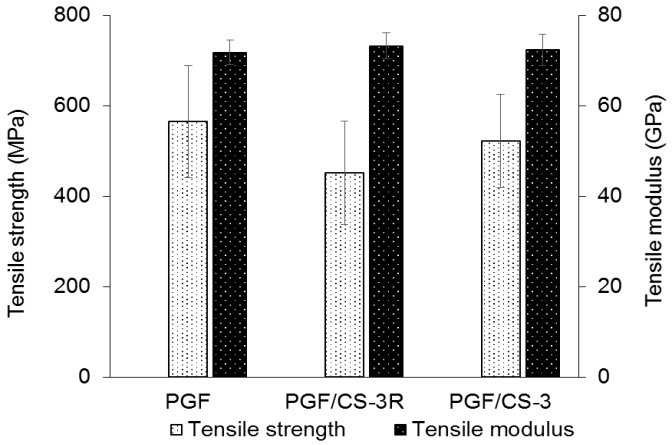

Figure 1: Mechanical properties (tensile strength and modulus) of the fibres ($n = 30$).

Table 2: Weibull parameters of the fibres ($n = 30$). The tensile strength values are also included for the ease of comparison.

Sample codes	Tensile strength (MPa)	Normalising strength (MPa)	Weibull modulus
PGF	565 ± 124	613	5.46
PGF/CS-3R	451 ± 114	495	5.47
PGF/CS-3	522 ± 104	565	5.27

3.2 IFSS

The fragmentation test showed a significant increase in IFSS after sizing ($p < 0.001$). The increments were 78.4% (4.38 MPa) and 56.0% (3.13 MPa) of the control for PGF/CS-3R and PGF/CS-3, respectively (see Figure 2**Error! Reference source not found.**). It was shown that the rinsing treatment increased the IFSS.

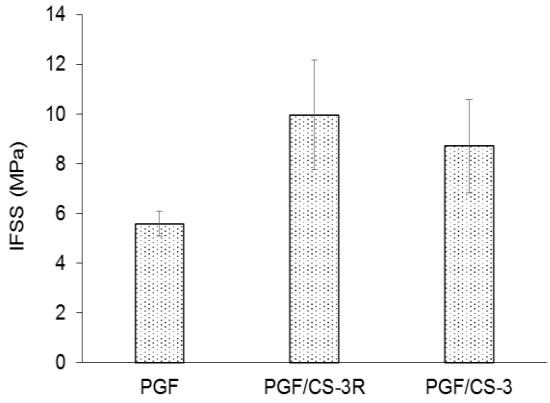

Figure 2: Interfacial shear stress (IFSS) values of the SFCs (n = 10).

3.3 SEM

It can be seen in Figure 3a that the untreated PGF had a smooth surface. The roughened fibre surface after treatment indicated the presence of sizing agents (see images b and c). The difference in surface condition between images b and c represented the effect of the rinsing process, which removed major excess CS without any visible acid corrosion on the fibre surface.

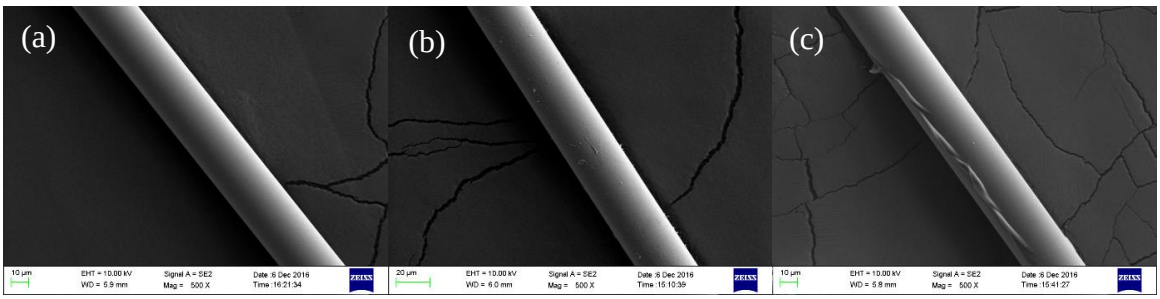

Figure 3: SEM images of (a) PGF, (b) PGF/CS-3R and (c) PGF/CS-3.

3.4 TG

The TG trace in Figure 4a shows a rapid weight loss at 310 °C for pure CS powder during heating under nitrogen. A weight loss was also observed for the sample PGF/CS-3 at ~300 °C. However, no clear weight change was found for the pure PGF and the sample PGF/CS-3R.

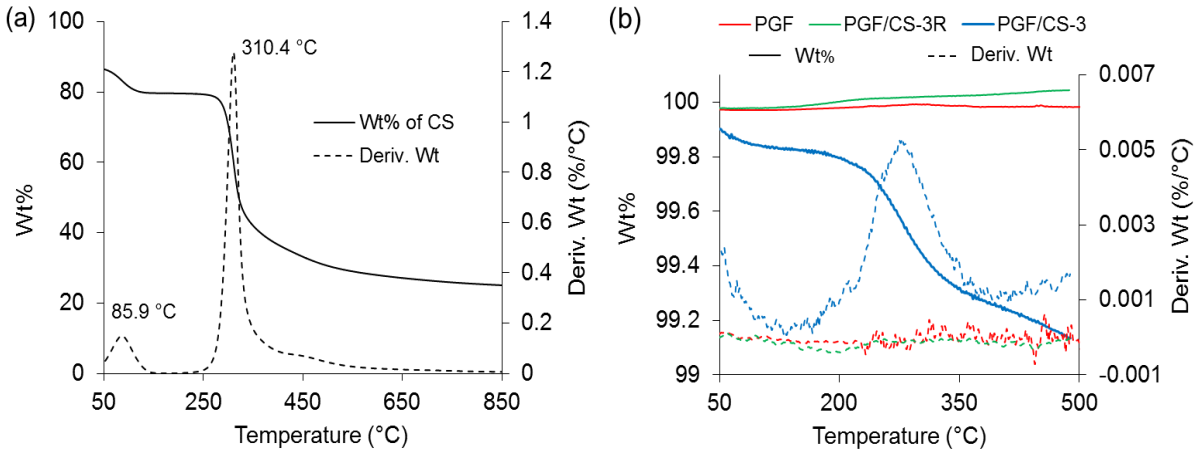

Figure 4: TG traces (weight percentage and derivative of weight percentage) of (a) CS powder and (b) sized and unsized PGFs.

3.5 XPS

High-resolution XPS spectroscopy was performed and the narrow scans of C_{1s}, N_{1s}, O_{1s}, P_{2p} and B_{1s} are shown in Figure 5. In the narrow scans of CS powder, the C_{1s} spectrum was deconvoluted into three peaks at 284.8, 286.3 and 287.8 eV binding energy; the N_{1s} spectrum was deconvoluted into two peaks at 399.4 and 401.0 eV; and the O_{1s} spectrum was deconvoluted into three peaks at 531.1, 532.6 and 533.9 eV. In the narrow scans of unsized PGF, the P_{2p} spectrum was deconvoluted into two peaks at 133.3 and 134.1 eV and the O_{1s} spectrum was deconvoluted into two peaks at 530.9 and 532.1 eV.

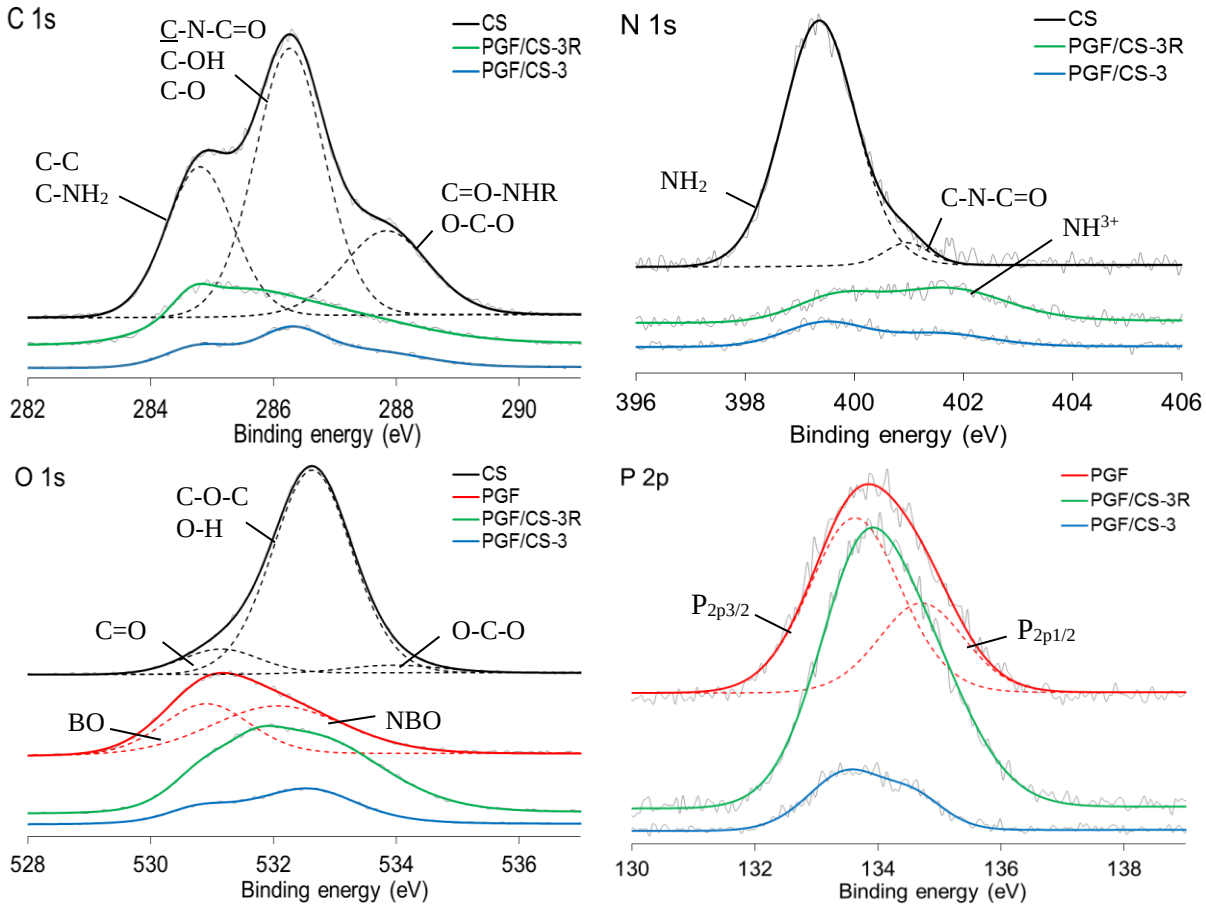

Figure 5: XPS C_{1s}, N_{1s}, O_{1s}, and P_{2p} narrow scans of CS powder and sized and unsized PGFs.

4 DISCUSSION

As shown in Figure 1, the dip-coating in the sizing solution led to an insignificant decrease ($p > 0.05$) in tensile strength of the fibres, while the rinsing in the acetic acid solution resulted in a significant strength loss ($p < 0.001$) compared to the control, which was suggested to be due to the acid-catalyzed hydrolysis on the glass (overall the 'rinsed' fibres spent twice as long in the acid solution) [32-35].

IFSS between the PCL matrix and PGF filament was observed to significantly increase ($p < 0.001$) after CS sizing. The rinsing process was employed to remove the extra agent on the fibre surface and consequently improved the interphase and load transmission between the matrix and fibres [12, 36]. No clear evidence of any significant increase in fibre roughness was obtained from the morphologic examination, e.g., no pitting corrosion was discovered on the surface of the rinsed fibres (see Figure 3b).

Zawadzki et al. [37] performed TG analysis of CS from room temperature to 600 °C under a nitrogen atmosphere and they described the TG behavior of CS in three stages: (1) the removal of water below 100 °C, in which the water was physically adsorbed and/or weakly hydrogen-bonded to CS molecules; (2) the release of strongly hydrogen-bonded water starting above 100 °C and reaching the maximum rate at ~168 °C and (3) the predominant weight loss at 230-400 °C caused by depolymerisation of CS chains, decomposition of pyranose rings through dehydration and deamination and finally ring-opening reaction [22, 38-40]. As can be seen, the TG trace of CS powder in Figure 4a shows a good agreement with the references. Moreover, the TG trace of PGF/CS-3 presented a distinct weight loss around 300 °C, while this phenomenon was not found for PGF/CS-3R, which was suggested that the rising treatment removed most of the sizing agents on the fibre surface. This is also consistent with the observation from SEM (see Figure 3). However, XPS shows that at least a small layer of the CS does remain on the fibre after rinsing. As shown in Figure 5, the C_{1s} spectrum of CS was resolved into three peaks, which showed a good agreement with others' work [41, 42]. The peak at 284.8 eV was assigned to C-C and C-NH_2; the peak at 286.3 eV was assigned to C-O, C-OH and C-N-C=O; and the peak at 287.8 eV was assigned to O-C-O and C=O-NHR [42, 43]. The C_{1s} spectrum of PGF/CS-3 was observed to have a similar shape with that of CS, which indicated the presence of CS on the PGF surface. The peak around 284.8 eV with high intensity in the C_{1s} spectrum of PGF/CS-3R was attributed to the prominence of C-C bonding after the removal of extra CS agent on the fibre surface, which was suggested to indicate the bonding of the CS to the PGF surface through the oxygen functionalities. In addition, although the intensities of the carbon peaks changed, no distinct peak shifting was observed for all the peaks.

The N_{1s} spectrum of CS showed one main peak at 399.4 eV for amine and another small peak at 401.0 eV for amide [41, 43-46]. The area of the former peak took 95% of the whole peak area. Lawrie et al. [46] have performed XPS for CS powders obtained from Sigma with a reported degree of deacetylation of 85%, which is quite similar to the material used in this paper. They focused on the spectrum of N_{1s} and identified it as one main signal at 399.4 eV with another negligible signal at 400.5 eV, corresponding to amine and amide, respectively. They subsequently characterised the acid treated CS film and detected one more signal at 401.4 eV, which was assigned to the protonated amine. As shown in Figure 5, a peak for the protonation of amino groups was also detected at 401.6 eV for PGF/CS-3 [43] and the area of NH^{3+} peak took 40% of the whole peak areas. After removal of extra sizing agents by the rinsing process, the area of NH^{3+} peak increased to 65% (see the N_{1s} spectrum of PGF/CS-3R in Figure 5).

The O_{1s} spectrum of CS was resolved into one main peak at 532.6 eV and two weak peaks at 531.1 and 533.9 eV. The peak with high intensity at 532.6 eV was assigned to C-O-C, O-H or bound water, and the weak peaks at 531.5 and 533.9 eV were assigned to C=O in amide groups and O-C-O in pyranose ring, respectively [41, 43-46]. The O_{1s} spectrum of PGF was deconvoluted into two peaks, which were seen at 530.9 and 532.1 eV binding energy for non-bridging (NBO) and bridging (BO) phosphate oxygen, respectively [47]. Majjane et al. [48], Salim et al. [49] and Haque et al. [12] have used XPS to investigate phosphate glass in the systems of P_2O_5-BaO-V_2O_5, P_2O_5-Fe_2O_3-V_2O_5 and P_2O_5-MgO-CaO-Na_2O-Fe_2O_3, respectively. All of them found a broad peak at ~531.0 eV in O_{1s} spectra and attributed this peak to the combination of BO and NBO. As shown in Figure 5, the highest intensity of O_{1s} peak for PGF/CS-3 was found at 532.6 eV binding energy, which was attributed to the CS agent; while the highest intensity of O_{1s} peak for PGF/CS-3R appeared around 531.9 eV, which was attributed to the overlapping of PGF and CS spectra. However, it is not possible to differentiate between the BO and NBO of the phosphate glass and the C-O-C and C=O bonds within the sizing agents, as both have absorption peaks over similar ranges of binding energy.

The P_{2p} spectrum of PGF was composed of the $P_{2p3/2}$/$P_{2p1/2}$ doublet and fitted with an energy difference of 1.1 eV and an approximate area ratio of 2:1. The peak of $P_{2p3/2}$ at 133.6 eV was attributed to pentavalent tetra coordinated phosphorus (pyrophosphate and orthophosphate) surrounded by a different chemical environment (phosphate-like structure) and the peak of $P_{2p1/2}$ at 134.7 eV was attributed to metaphosphate [48, 50, 51]. The spectrum of PGF/CS-3R was resolved into two peaks at 133.7 and 134.8 eV with an approximate area ratio of 2:1, while the spectrum of PGF/CS-3 was

resolved into two peaks at 133.5 and 134.6 eV with an approximate area ratio of 2.6:1. A shift of binding energy was observed for P_{2p} after the process of sizing and rinsing. Combining the varying binding energy of N_{1s}, it was suggested that there was an electronic interaction between the protonated amine and the PGF surface [52]. However, it was difficult for a deeper analysis of the interaction due to the overlapping of binding energies in the O_{1s} spectra of CS and PGF.

Positively charged amine groups (NH^{3+}) are generated via protonation when CS is dissolved in weak acid solution [53], which allows for pH-dependent electrostatic interactions between CS and any negatively charged species in a manner similar to amino silane [24, 54, 55]. In this case, the protonation of amino groups has been demonstrated by XPS. Therefore, the charged CS has the possibility of interacting with the $[PO_4]^-$ group of the PGF. Huang et al. [23] added glycerol-phosphate to the CS-acetic acid solution and found the interaction caused by the electrostatic attractions via NH^{3+} and P-OH groups between CS and glycerol-phosphate. Chenite et al. [56] summarised that the combination of CS and polyol-phosphate salts can form hydrogen bonding, electrostatic interactions and hydrophobic interactions in acetic acid solution. Due to the structural similarity with polyol-phosphate [34, 57], PGF has the possibility to occur the similar interactions with CS. Amaral et al. [43] investigated the phosphorylation of CS using XPS and also assigned the signal at 401.4 eV in the N_{1s} spectrum to amino groups in ammonium form [58]. They proposed that the phosphate groups and protonated amine groups were likely to form salt linkages with inter- or intra-chain ionic bonds [59]. Zhang et al. reinforced a CS scaffold with P_2O_5-CaO invert glass and suggested that the chemical attraction between CS and the glass might take place due to the high surface charge density of CS [29]. Furthermore, the hydroxyl functional groups in CS have the potential to react with the glass through the hydroxyl groups present on PGF surface [34, 60]. The interactions described above are believed to improve IFSS and as a result, infer better load transfer from the matrix to fibres [34].

5 CONCLUSIONS

TGA and SEM indicated the presence of CS agent on the PGF surface. CS was shown to be able to improve the fibre/matrix interface of PGF/PCL composites by 56%. The post-treatment cleaning step enhanced the IFSS but incurred a tensile strength loss of 20% for the sized fibres. The XPS analysis suggested that the enhancement of the interfacial property was due to the interaction between the protonated amine groups of the CS and the phosphate structure of the PGF.

ACKNOWLEDGEMENTS

This work was carried out at the International Doctoral Innovation Centre (IDIC). The authors acknowledge the financial support from Ningbo Education Bureau, Ningbo Science and Technology Bureau, China's MOST and The University of Nottingham. The work is also partially supported by EPSRC (Grant no. EP/L016362/1). The authors would also like to acknowledge the financial support from Ningbo 3315 Innovation team Scheme “Composites Development and Manufacturing for Sustainable Environment”.

REFERENCES

[1] S. Cozien-Cazuc, A. J. Parsons, G. S. Walker, I. A. Jones, and C. D. Rudd, "Real-time dissolution of P40Na20Ca16Mg24 phosphate glass fibers," *J Non Cryst Solids*, vol. 355, pp. 2514-2521, 2009.

[2] R. A. Khan, A. J. Parsons, I. A. Jones, G. S. Walker, and C. D. Rudd, "Degradation and Interfacial Properties of Iron Phosphate Glass Fiber-Reinforced PCL-Based Composite for Synthetic Bone Replacement Materials," *Polym-Plast Technol*, vol. 49, pp. 1265-1274, 2010.

[3] R. M. Felfel, I. Ahmed, A. J. Parsons, G. Palmer, V. Sottile, and C. D. Rudd, "Cytocompatibility, degradation, mechanical property retention and ion release profiles for

phosphate glass fibre reinforced composite rods," *Mater Sci Eng C Mater Biol Appl,* vol. 33, pp. 1914-24, May 1 2013.

[4] C. Tan, I. Ahmed, A. J. Parsons, N. Sharmin, C. Zhu, J. Liu, *et al.*, "Structural, thermal and dissolution properties of MgO- and CaO-containing borophosphate glasses: effect of Fe2O3 addition," *J Mater Sci,* vol. 52, pp. 7489-7502, 2017.

[5] A. J. Parsons, I. Ahmed, P. Haque, B. Fitzpatrick, M. I. K. Niazi, G. S. Walker, *et al.*, "Phosphate Glass Fibre Composites for Bone Repair," *J Bionic Eng,* vol. 6, pp. 318-323, 2009.

[6] M. Bitar, V. Salih, V. Mudera, J. C. Knowles, and M. P. Lewis, "Soluble phosphate glasses: in vitro studies using human cells of hard and soft tissue origin," *Biomaterials,* vol. 25, pp. 2283-2292, 2004.

[7] A. J. Parsons, M. Evans, C. D. Rudd, and C. A. Scotchford, "Synthesis and degradation of sodium iron phosphate glasses and their in vitro cell response," *J Biomed Mater Res A,* vol. 71, pp. 283-91, Nov 1 2004.

[8] C. Zhu, I. Ahmed, A. Parsons, K. Z. Hossain, C. Rudd, J. Liu, *et al.*, "Structural, thermal, in vitro degradation and cytocompatibility properties of P2O5-B2O3-CaO-MgO-Na2O-Fe2O3 glasses," *Journal of Non-Crystalline Solids,* vol. 457, pp. 77-85, 2017.

[9] I. Ahmed, I. A. Jones, A. J. Parsons, J. Bernard, J. Farmer, C. A. Scotchford, *et al.*, "Composites for bone repair: phosphate glass fibre reinforced PLA with varying fibre architecture," *J Mater Sci-Mater M,* vol. 22, pp. 1825-1834, 2011.

[10] N. Sharmin, A. J. Parsons, C. D. Rudd, and I. Ahmed, "Effect of boron oxide addition on fibre drawing, mechanical properties and dissolution behaviour of phosphate-based glass fibres with fixed 40, 45 and 50 mol% P_2O_5," *J Biomater Appl,* vol. 29, pp. 639-53, Nov 2014.

[11] A. Anitha, S. Sowmya, P. T. S. Kumar, S. Deepthi, K. P. Chennazhi, H. Ehrlich, *et al.*, "Chitin and chitosan in selected biomedical applications," *Prog Polym Sci,* vol. 39, pp. 1644-1667, 2014.

[12] P. Haque, A. J. Parsons, I. A. Barker, I. Ahmed, D. J. Irvine, G. S. Walker, *et al.*, "Interfacial properties of phosphate glass fibres/PLA composites: Effect of the end functionalities of oligomeric PLA coupling agents," *Compos Sci Technol,* vol. 70, pp. 1854-1860, 2010.

[13] M. S. Hasan, I. Ahmed, A. J. Parsons, G. S. Walker, and C. A. Scotchford, "The influence of coupling agents on mechanical property retention and long-term cytocompatibility of phosphate glass fibre reinforced PLA composites," *J Mech Behav Biomed Mater,* vol. 28, pp. 1-14, Dec 2013.

[14] M. S. Mohammadi, I. Ahmed, N. Muja, C. D. Rudd, M. N. Bureau, and S. N. Nazhat, "Effect of phosphate-based glass fibre surface properties on thermally produced poly(lactic acid) matrix composites," *J Mater Sci Mater Med,* vol. 22, pp. 2659-72, Dec 2011.

[15] X. Liu, D. M. Grant, G. Palmer, A. J. Parsons, C. D. Rudd, and I. Ahmed, "Magnesium coated phosphate glass fibers for unidirectional reinforcement of polycaprolactone composites," *J Biomed Mater Res B Appl Biomater,* vol. 103, pp. 1424-32, Oct 2015.

[16] X. Geng, O. H. Kwon, and J. Jang, "Electrospinning of chitosan dissolved in concentrated acetic acid solution," *Biomaterials,* vol. 26, pp. 5427-32, Sep 2005.

[17] D. W. Lee, H. Lim, H. N. Chong, and W. S. Shim, "Advances in Chitosan Material and its Hybrid Derivatives: A Review," *The Open Biomaterials Journal,* vol. 1, pp. 10-29, 2009.

[18] R. Mad Jin, N. Sultana, S. Baba, S. Hamdan, and A. F. Ismail, "Porous PCL/Chitosan and nHA/PCL/Chitosan Scaffolds for Tissue Engineering Applications: Fabrication and Evaluation," *J Nanomater,* vol. 2015, pp. 1-8, 2015.

[19] V. K. Mourya and N. N. Inamdar, "Chitosan-modifications and applications: Opportunities galore," *React Funct Polym,* vol. 68, pp. 1013-1051, 2008.

[20] Z. Osman and A. K. Arof, "FTIR studies of chitosan acetate based polymer electrolytes," *Electrochim Acta,* vol. 48, pp. 993-999, 2003.

[21] H. Kweon, I. C. Um, and Y. H. Park, "Structural and thermal characteristics of Antheraea pernyi silk fibroin/chitosan blend film," *Polymer,* vol. 42, pp. 6651–6656, 2001.

[22] R. Ramya, P. N. Sudha, and J.Mahalakshmi, "Preparation and Characterization of Chitosan Binary Blend," *International Journal of Scientific and Research Publications,* vol. 2, pp. 1-9, 2012.

[23] C. L. Huang, Y. B. Chen, Y. L. Lo, and Y. H. Lin, "Development of chitosan/beta-glycerophosphate/glycerol hydrogel as a thermosensitive coupling agent," *Carbohyd Polym*, vol. 147, pp. 409-14, Aug 20 2016.

[24] B. L. Shah, L. M. Matuana, and P. A. Heiden, "Novel coupling agents for PVC/wood-flour composites," *J Vinyl Addit Techn*, vol. 11, pp. 160-165, 2005.

[25] X. Cai, H. Tong, X. Shen, W. Chen, J. Yan, and J. Hu, "Preparation and characterization of homogeneous chitosan-polylactic acid/hydroxyapatite nanocomposite for bone tissue engineering and evaluation of its mechanical properties," *Acta Biomater*, vol. 5, pp. 2693-703, Sep 2009.

[26] D. H. Min, M. J. Kim, J. H. Yun, C. S. Kim, Y.-K. Lee, S. H. Choi, *et al.*, "Effect of Calcium Phosphate Glass Scaffold with Chitosan Membrane on the Healing of Alveolar Bone in 1 Wall Intrabony Defect in the Beagle Dogs," *Key Engineering Materials*, vol. 284-286, pp. 851-854, 2005.

[27] A. Sarasam and S. V. Madihally, "Characterization of chitosan-polycaprolactone blends for tissue engineering applications," *Biomaterials*, vol. 26, pp. 5500-8, Sep 2005.

[28] N. Bhattarai, Z. Li, J. Gunn, M. Leung, A. Cooper, D. Edmondson, *et al.*, "Natural-Synthetic Polyblend Nanofibers for Biomedical Applications," *Adv Mater*, vol. 21, pp. 2792-2797, 2009.

[29] Y. Zhang and M. Zhang, "Microstructural and mechanical characterization of chitosan scaffolds reinforced by calcium phosphates," *J Non Cryst Solids*, vol. 282, pp. 159-164, 2001.

[30] E. A. El-Hefian, M. M. Nasef, and A. H. Yahaya, "The Preparation and Characterization of Chitosan/Poly (Vinyl Alcohol) Blended Films," *E-J Chem*, vol. 7, pp. 1212-1219, 2010.

[31] I. Ahmed, A. J. Parsons, G. Palmer, J. C. Knowles, G. S. Walker, and C. D. Rudd, "Weight loss, ion release and initial mechanical properties of a binary calcium phosphate glass fibre/PCL composite," *Acta Biomater*, vol. 4, pp. 1307-14, Sep 2008.

[32] M. Shokrieh, V. Nasir, and H. Karimipour, "Strength behavior and crack-formation mechanisms of E-glass fiber exposed to sulfuric acid environment," *J Compos Mater*, vol. 46, pp. 765-772, 2011.

[33] R. L. Jones and J. Stewart, "The kinetics of corrosion of e-glass fibres in sulphuric acid," *J Non Cryst Solids*, vol. 356, pp. 2433-2436, 2010.

[34] M. S. Hasan, I. Ahmed, A. Parsons, G. Walker, and C. Scotchford, "Cytocompatibility and Mechanical Properties of Short Phosphate Glass Fibre Reinforced Polylactic Acid (PLA) Composites: Effect of Coupling Agent Mediated Interface," *J Funct Biomater*, vol. 3, pp. 706-25, 2012.

[35] H. Gao, T. Tan, and D. Wang, "Dissolution mechanism and release kinetics of phosphate controlled release glasses in aqueous medium," *J Control Release*, vol. 96, pp. 29-36, Apr 16 2004.

[36] M. S. Hasan, I. Ahmed, A. J. Parsons, C. D. Rudd, G. S. Walker, and C. A. Scotchford, "Investigating the use of coupling agents to improve the interfacial properties between a resorbable phosphate glass and polylactic acid matrix," *J Biomater Appl*, vol. 28, pp. 354-66, Sep 2013.

[37] J. Zawadzki and H. Kaczmarek, "Thermal treatment of chitosan in various conditions," *Carbohyd Polym*, vol. 80, pp. 394-400, 2010.

[38] M. Bengisu and E. Yilmaz, "Oxidation and pyrolysis of chitosan as a route for carbon fiber derivation," *Carbohyd Polym*, vol. 50, pp. 165–175, 2002.

[39] T. Wanjun, W. Cunxin, and C. Donghua, "Kinetic studies on the pyrolysis of chitin and chitosan," *Polym Degrad Stabil*, vol. 87, pp. 389-394, 2005.

[40] A. Pawlak and M. Mucha, "Thermogravimetric and FTIR studies of chitosan blends," *Thermochim Acta*, vol. 396, pp. 153–166, 2003.

[41] Y. M. Nikolenko, V. G. Kuryavyi, I. V. Sheveleva, L. A. Zemskova, and V. I. Sergienko, "Atomic force microscopy and X-ray photoelectron spectroscopy study of chitosan-carbon fiber materials," *Inorganic Materials*, vol. 46, pp. 221-225, 2010.

[42] W. F. Yap, W. M. M. Yunus, Z. A. Talib, and N. A. Yusof, "X-ray photoelectron spectroscopy and atomic force microscopy studies on crosslinked chitosan thin film," *International Journal of the Physical Sciences* vol. 6, pp. 2744-2749, 4 June 2011.

[43] I. F. Amaral, P. L. Granja, and M. A. Barbosa, "Chemical modification of chitosan by phosphorylation: an XPS, FT-IR and SEM study," *Journal of Biomaterials Science, Polymer Edition*, vol. 16, pp. 1575–1593, 2005.

[44] S. Danielache, M. Mizuno, S. Shimada, K. Endo, T. Ida, K. Takaoka, *et al.*, "Analysis of 13C NMR Chemical Shielding and XPS for Cellulose and Chitosan by DFT Calculations Using the Model Molecules," *Polymer Journal*, vol. 37, pp. 21-29, 2005.

[45] A. K. Arof, N. M. Morni, and M. A. Yarmo, "Evidence of lithium–nitrogen interaction in chitosan-based films from X-ray photoelectron spectroscopy," *Materials Science and Engineering: B*, vol. 55, pp. 130–133, 1998.

[46] G. Lawrie, I. Keen, B. Drew, A. Chandler-Temple, L. Rintoul, P. Fredericks, *et al.*, "Interactions between Alginate and Chitosan Biopolymers Characterized Using FTIR and XPS," *Biomacromolecules*, vol. 8, pp. 2533-2541, 2007.

[47] R. Gresch and W. Müller-Warmuth, "X-ray photoelectron spectroscopy of sodium phosphate glasses," *J Non Cryst Solids*, vol. 34, pp. 127-136, 1979.

[48] A. Majjane, A. Chahine, M. Et-tabirou, B. Echchahed, T.-O. Do, and P. M. Breen, "X-ray photoelectron spectroscopy (XPS) and FTIR studies of vanadium barium phosphate glasses," *Materials Chemistry and Physics*, vol. 143, pp. 779-787, 2014.

[49] M. A. Salim, G. D. Khattak, P. S. Fodor, and L. E. Wenger, "X-ray photoelectron spectroscopy (XPS) and magnetization studies of iron–vanadium phosphate glasses," *Journal of Non-Crystalline Solids*, vol. 289, pp. 185-195, 2001.

[50] A. M. Puziy, O. I. Poddubnaya, R. P. Socha, J. Gurgul, and M. Wisniewski, "XPS and NMR studies of phosphoric acid activated carbons," *Carbon*, vol. 46, pp. 2113-2123, 2008.

[51] M. Pelavin, D. N. Hendrickson, J. M. Hollander, and W. L. Jolly, "Phosphorus 2p electron binding energies. Correlation with extended Hueckel charges," *The Journal of Physical Chemistry* vol. 74, pp. 1116–1121, 1970.

[52] J. Liu, S. Zou, L. Xiao, and J. Fan, "Well-dispersed bimetallic nanoparticles confined in mesoporous metal oxides and their optimized catalytic activity for nitrobenzene hydrogenation," *Catal. Sci. Technol.*, vol. 4, pp. 441-446, 2014.

[53] J. Berger, M. Reist, J. M. Mayer, O. Felt, N. A. Peppas, and R. Gurny, "Structure and interactions in covalently and ionically crosslinked chitosan hydrogels for biomedical applications," *Eur J Pharm Biopharm*, vol. 57, pp. 19-34, 2004.

[54] S. V. Madihally and H. W. T. Matthew, "Porous chitosan scaffolds for tissue engineering," *Biomaterials*, vol. 20, pp. 1133-1142, 1999.

[55] C. J. Knill, J. F. Kennedy, J. Mistry, M. Miraftab, G. Smart, M. R. Groocock, *et al.*, "Alginate fibres modified with unhydrolysed and hydrolysed chitosans for wound dressings," *Carbohyd Polym*, vol. 55, pp. 65-76, 2004.

[56] A. Chenite, C. Chaput, D. Wang, C. Combes, M. D. Buschmann, C. D. Hoemann, *et al.*, "Novel injectable neutral solutions of chitosan form biodegradable gels in situ," *Biomaterials*, vol. 21, pp. 2155–2161, 2000.

[57] P. Haque, I. A. Barker, A. Parsons, K. J. Thurecht, I. Ahmed, G. S. Walker, *et al.*, "Influence of compatibilizing agent molecular structure on the mechanical properties of phosphate glass fiber-reinforced PLA composites," *J Polym Sci Pol Chem*, vol. 48, pp. 3082-3094, 2010.

[58] B. Lindberg, R. Maripuu, K. Siegbahn, R. Larsson, C.-G. Gölander, and J. C. Eriksson, "ESCA Studies of heparinized and related surfaces: 1. Model surfaces on steel substrates," *Journal of Colloid and Interface Science* vol. 95, pp. 308-321, 1983.

[59] N. Nishi, A. Ebina, S.-i. Nishimura, A. Tsutsumi, O. Hasegawa, and S. Tokura, "Highly phosphorylated derivatives of chitin, partially deacetylated chitin and chitosan as new functional polymers: preparation and characterization," *International Journal of Biological Macromolecules*, vol. 8, pp. 311-317, 1986.

[60] C. K. S. Pillai, W. Paul, and C. P. Sharma, "Chitin and chitosan polymers: Chemistry, solubility and fiber formation," *Prog Polym Sci*, vol. 34, pp. 641-678, 2009.